Desalination and Water Treatment
www.deswater.com

doi:10.5004/dwt.2019.24169

159 (2019) 310–317
August

Influences of cetyltrimethyl ammonium bromide template on photocatalytic degradation of ofloxacin on porous $La_2Ti_2O_7$

Yan Wang, Yue Zhang, Zheng Ma, Wenjie Zhang*

School of Environmental and Chemical Engineering, Shenyang Ligong University, Shenyang 110159, China, email: 1792841456@qq.com (Y. Wang), 843175987@qq.com (Y. Zhang), 497783652@qq.com (Z. Ma), Tel. +86-13609880790, email: wjzhang@aliyun.com (W. Zhang)

Received 21 September 2018; Accepted 21 March 2019

ABSTRACT

Porous $La_2Ti_2O_7$ photocatalyst was synthesized by sol-gel method using cetyltrimethyl ammonium bromide (CTAB) as the template. Ofloxacin degradation mechanism and the effects of CTAB on photocatalytic activity of the porous $La_2Ti_2O_7$ were examined. The addition of CTAB in preparation of $La_2Ti_2O_7$ can obviously enhance the activity of the material, and the first order reaction rate constants are 0.0128, 0.0187 and 0.0245 min^{-1} on the $La_2Ti_2O_7$ samples obtained using 0, 2 and 4 g of CTAB, respectively. Photocatalytic degradation efficiency is almost linearly enhanced with the increase of $La_2Ti_2O_7$ dosage in less than 300 mg/L. When the $La_2Ti_2O_7$ sample obtained using 4 g CTAB was used, total organic carbon in the solution is reduced from 20.9 mg/L to 5.1 mg/L after 120 min of irradiation. The functional groups in ofloxacin molecule are decomposed during photocatalytic oxidation, which are proven by the shrinking absorption intensities in both UV-Visible and FT-IR spectra. F^-, NH_4^+ and NO_2^- ions in the solution continuously increase with extending irradiation time, showing the separation of fluoride ion and nitrogen from ofloxacin molecule.

Keywords: Lanthanum titanate; Heterogeneous photocatalysis; Cetyltrimethyl ammonium bromide; Ofloxacin; Degradation

1. Introduction

Wastewater containing antibiotics has aroused great attention for the big threat to human beings and the environment. The traditional bio-chemical treatment is hardly used for this kind of wastewater since the antibiotics are harmful to microorganisms. Photocatalytic technique has been studied for half a century for removing most kinds of organic pollutants from polluted air and water [1–3]. Photogenerated electrons and holes can be produced when photocatalyst is exposed to incoming irradiation with enough power, and subsequent oxidation of organic substance will lead to decomposition of most environmental organic pollutants [4–6]. Recently, researchers reported the application of photocatalysts on photocatalytic oxidation of some types of antibiotics [7–11]. Hydroxyl and $\cdot O_2$ radicals can be produced during heterogeneous photocatalytic process and act as oxidative reagents to degrade many kinds of organic pollutants [12–14].

Photocatalyst is the most important factor that can determine the application of photocatalytic technique in wastewater treatment [15,16]. Although TiO_2-based material is the most studied photocatalyst, this kind of material still has disadvantages in large scale application [17,18]. Different strategies (doping, supporting, coupling) are adopted to increase the photocatalytic activity of semiconducting materials [19–21]. Titanates in pyrochloro and perovskite structure have also aroused special attention [22–26]. Strontium titanate and barium titanate were reported to be the photocatalysts for both hydrogen evolution and pollutants degradation [27–29]. We reported the enhanced activity of $Gd_2Ti_2O_7$ after supporting on HZSM-5 zeolite for the purpose of ofloxacin degradation [30]. Lanthanum titanate is among the potential titanate photocatalysts and has been reported for decomposition of organic pollutants [31,32].

*Corresponding author.

High temperature calcination is usually necessary for crystallization of titanate, so that particles aggregation and agglomeration may result in the formation of large particles without apparent porous structure. The addition of polyethylene glycol (PEG) in the precursor can introduce pores in titania for the enhanced photocatalytic activity. For example, Zhang et al. prepared TiO_2 nanowires with high specific surface area that was responsible for the high efficiency on atrazine degradation [33]; Chang et al. modified TiO_2-$InVO_4$ nanoparticles by PEG in a combustion synthesizing route [34]. However, the preparation of porous titanate with the help of template reagent is seldom reported in the literature. We firstly reported the PEG4000-mediated sol-gel synthesizing of porouscerium titanate [25,35] and the CTAB-mediated synthesis of porous $La_2Ti_2O_7$ [36].

The application of template reagent is still a novel topic in forming porous structure in titanate. Cetyltrimethyl ammonium bromide is a typical cationic quaternary amine, which can be used as surfactant and pore-forming reagent. Porous $La_2Ti_2O_7$ was prepared in a sol-gel route in which cetyltrimethyl ammonium bromide (CTAB) was used as the template, and the porous $La_2Ti_2O_7$ was used as photocatalyst for ofloxacin degradation in this work. The ofloxacin solution during photocatalytic degradation process was determined using Fourier transform infrared spectroscopy (FT-IR), UV-Visible spectrometry, total organic carbon analysis (TOC), and ion chromatography (IC). The purpose of this work was to examine ofloxacin degradation mechanism and to clarify the effects of CTAB addition.

2. Experimental

2.1. Preparation of porous $La_2Ti_2O_7$

All the chemicals used in this work were in analytical pure and were obtained from Sinopharm Chemical Reagent Co., Ltd. The sol-gel route contained the preparation of precursors and sol-gel transformation steps. One precursor was made from 8 mL deionized water, 1.0825 g lanthanum nitrate, 8 mL acetic acid and 0–9 g CTAB. Another precursor was made from 0.85 mL tetrabutyl titanate and 8 mL ethanol. The former precursor was dropped into the second precursor to ensure sol-gel transformation in a 70°C water bath. The sol-gel transformation time was controlled by adding 2 mL ethylene glycol into the mixture. The obtained gel was dehydrated at 110°C and therefore was calcined at 800°C for 3 h. The final $La_2Ti_2O_7$ product was ground into fine powders before use.

2.2. Photocatalytic degradation of ofloxacin

The porous $La_2Ti_2O_7$ samples were examined to compare the adsorption capacity and photocatalytic oxidation efficiency in a 100 mL quartz beaker. The illumination source was a 20 W ultraviolet lamp that could mainly irradiate at 253.7 nm at the intensity of 2300 μW/cm^2. 50 mL of 40 mg/L ofloxacin solution and 30 mg of $La_2Ti_2O_7$ were stirred in the dark to examine the adsorption capacity of the material. Subsequently, the UV lamp was turned on to start the degradation of ofloxacin. Ofloxacin concentration was measured using Agilent 1260 high performance liquid chromatography equipped with a ZorbaxEclipse XDB-C18 (150×4.6 mm, 5 μm) column. The mobile phase was made from 1% phosphoric acid aqueous solution and acetonitrile at a volume ratio of 80:20. The flow rate of the mobile phase was 1.2 mL/min. The absorption intensity of ofloxacin at 288 nm was detected by a UV detector.

2.3. Determination of ofloxacin solution

The mixture of ofloxacin solution and $La_2Ti_2O_7$ photocatalyst was centrifuged for 10 min at 11000 rpm and was filtrated through a 0.45 μm Millipore filter to remove the solid before the determinations of Fourier transform infrared spectroscopy, UV-Visible spectrometry, total organic carbon, and ion chromatography. Subsequently, 15 mL of the ofloxacin solution was evaporated at 40°C to remove water. The obtained solid was dissolved in 1 mL methane, followed by addition of 100 mg KBr. The mixture of KBr and methane solution was dried at 30°C to remove methane, before taking infrared spectrum by a Frontier FT-IR/FIR spectrometer. UV-Vis spectrum of the ofloxacin solution was recorded by LAMBDA 35 UV-Vis spectrometer. The scanning speed was 480 nm/min in the wavelength range between 200 and 800 nm. Total organic carbon analysis of the ofloxacin solution was measured by Analytikjenamulti N/C 3100 TOC/TN analyzer. The combustion furnace temperature was 850°C. The concentrations of F^-, NH_4^+, NO_2^- and NO_3^- ions were determined by ICS1100 ion chromatograph, which was equipped with AERS 500 (4 mm) anion suppressor, CERS 500 (4 mm) cation suppressor, IonPac AS11-HC (4×250 mm) anion analytical column and CS12A (4 mm) cation analytical column. The flow rate of the mobile phase was 1 mL/min, and the injection volume was 10 μL. The ofloxacin solution was pretreated using a RP-C18 column to remove the organic substances in the solution.

3. Results and discussion

3.1. Photocatalytic degradation of ofloxacin

Detailed characterization results of the porous $La_2Ti_2O_7$ material were reported in our previous work [36]. Here, the role of CTAB on synthesizing and properties of $La_2Ti_2O_7$ can be briefly expressed. The materials are composed of perovskite $La_2Ti_2O_7$ in monoclinic system. The addition of CTAB does not cause phase transformation, but leads to a slight decreasing tendency of $La_2Ti_2O_7$ crystallite size. The concentration of CTAB in the precursor is more than the first and second critical micelle concentration of CTAB [37,38]. Tetrabutyl titanate molecules are adhered on the macromolecular CTAB, followed by subsequent hydrolysis of tetrabutyl titanate. The aggregation of small $La_2Ti_2O_7$ particles is reduced after using CTAB. BET specific surface area, average pore size and total pore volume of the $La_2Ti_2O_7$ particles are enlarged after using CTAB template.

Fig. 1 compares photocatalytic ofloxacin degradation efficiency on the porous $La_2Ti_2O_7$ samples with the variation of CTAB amount in the precursor. Adsorption percentage of ofloxacin on the materials is also shown in Fig. 1a. About 10% of the initial ofloxacin molecules in the solution

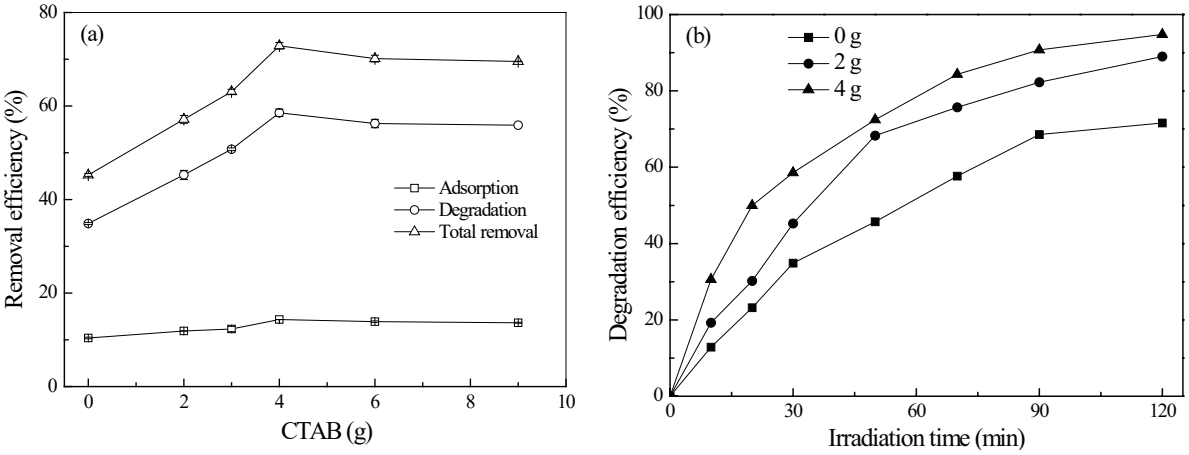

Fig. 1. Adsorption and photocatalytic degradation of ofloxacin on the porous $La_2Ti_2O_7$ samples. (a) Adsorption and photocatalytic degradation efficiency after 30 min of irradiation as a factor of CTAB amount, (b) Degradation of ofloxacin with prolonged irradiation time on different porous $La_2Ti_2O_7$ samples.50 mL of 40 mg/L ofloxacin solution and 30 mg of $La_2Ti_2O_7$ were used.

can be removed through adsorption on the materials, which was measured after adsorption and desorption of ofloxacin reached equilibrium. The adsorption percent is slightly enhanced after adding CTAB in the precursor, while it becomes constant after adding 4 g of CTAB to prepare $La_2Ti_2O_7$. Although as much as 14% of the initial ofloxacin molecules can be removed from the solution by adsorption, it cannot lead to decomposition of the hazardous drug.

Photocatalytic oxidation is effective in breaking ofloxacin molecule up into fragments, resulting in different kinds of intermediates and final products. As can be seen from Fig. 1a, the addition of CTAB in preparation of $La_2Ti_2O_7$ can obviously enhance the activity of the material. The degradation efficiency in 30 min is 35% when the $La_2Ti_2O_7$ sample obtained without CTAB is used, and it is linearly increased to 58.6% when CTAB amount is less than 4 g. After that, the degradation efficiency does not continuously increase with rising CTAB amount. As shown in Fig. 1(b), photocatalytic degradation of ofloxacin obeys the first order reaction law. When the $La_2Ti_2O_7$ sample obtained using 4 g of CTAB is used, ofloxacin molecules are not detectable after 120 min of irradiation in the solution since all the remaining ofloxacin molecules are degraded. According to Langmuir–Hinshelwood equation [39,40], $r = -dc/dt = k\theta = k(KC/(1+KC))$, the first order reaction rate constants are 0.0128, 0.0187 and 0.0245 min^{-1} on the $La_2Ti_2O_7$ samples obtained using 0, 2 and 4 g of CTAB, respectively.

$La_2Ti_2O_7$ dosage inofloxacin solution can influence both adsorption and photocatalytic degradation of ofloxacin molecules on the material, as presented in Fig. 2. The $La_2Ti_2O_7$ sample obtained using 4 g CTAB was used to determine the suitable photocatalyst dosage. The percent of ofloxacin molecules that is removed by adsorption constantly increases with rising $La_2Ti_2O_7$ dosage. Meanwhile, photocatalytic degradation efficiency is almost linearly enhanced with the increase of $La_2Ti_2O_7$ dosage in less than 300 mg/L. Photocatalytic degradation efficiency depends on the amount of incoming photons that can be absorbed by the photocatalyst. Normally, more photons can be absorbed at higher photocatalyst dosage. However, $La_2Ti_2O_7$ might aggregate into large particles at high dosage and therefore, the photocatalyst surface that is available to absorbing the photons is not as large as the highly dispersed small $La_2Ti_2O_7$ particles [41,42]. The optimal $La_2Ti_2O_7$ dosage in this work is 300 mg/L.

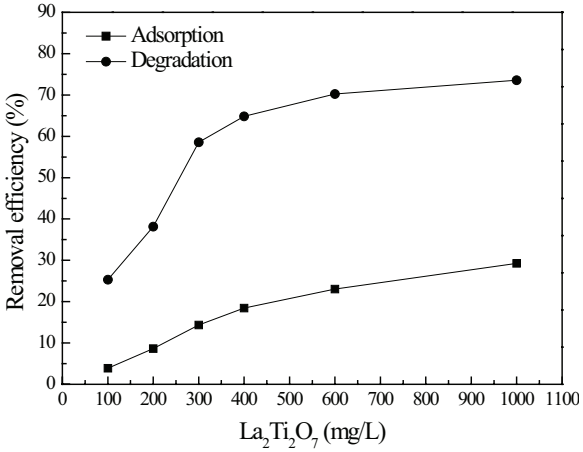

Fig. 2. Effect of $La_2Ti_2O_7$ dosage on ofloxacin degradation efficiency. The $La_2Ti_2O_7$ sample was prepared using 4 g CTAB. 50 mL of 40 mg/L ofloxacin solution was used.

TOC determination of the ofloxacin solution during photocatalytic degradation process is shown in Fig. 3. It is known that decomposition of ofloxacin in the initial photocatalytic degradation stage is followed by mineralization of the oxidation intermediates. The decreasing rate of total organic carbon in the solution depends on the activity of the materials. As stated before, the activity of $La_2Ti_2O_7$ is enhanced after adding CTAB in the synthesizing process. The TOC removal rate is in accordance to the activity of the porous $La_2Ti_2O_7$. When the $La_2Ti_2O_7$ sample obtained using 4 g CTAB was used, total organic carbon in the solution is reduced from 20.9 mg/L to 5.1 mg/L after 120 min of irradiation. It is mentioned that all the ofloxacin molecules are decomposed in the solution at this time, but the TOC removal efficiency is 75.6%. TOC removal rate becomes

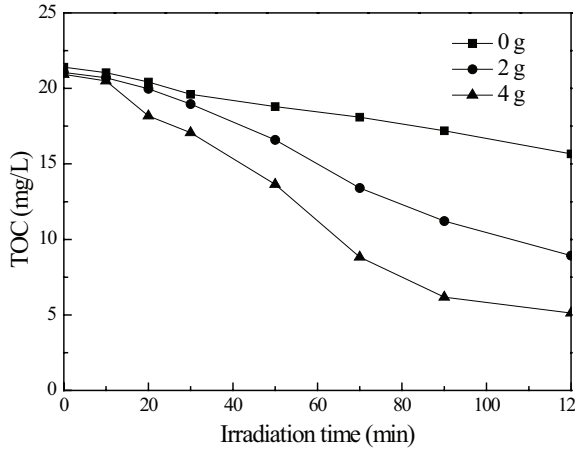

Fig. 3. TOC removal efficiency during photocatalytic degradation of ofloxacin solution with the existence of $La_2Ti_2O_7$ obtained using different amount of CTAB. 50 mL of 40 mg/L ofloxacin solution and 30 mg of $La_2Ti_2O_7$ were used.

slowly after 90 min of irradiation and there are still some organic substances remaining in the solution. Total mineralization of the remaining intermediates might be possible, but it must take more time.

3.2. UV-Vis and FT-IR spectra of ofloxacin solution

Fig. 4a presents UV-Vis spectra of ofloxacin solution during photocatalytic degradation in presence of $La_2Ti_2O_7$ sample obtained using 4 g CTAB. The ofloxacin molecule does not have absorptions in the visible region, while there are four absorption peaks in the ultraviolet region. The quinolone substituent of ofloxacin molecule has a strong absorption at 288 nm, which is characterized to measure the concentration of ofloxacin solution. The weak absorption peak at 255 nm is attributed to the π-π^* excitation in benzoic ring, and the piperazinyl and oxazinyl groups in ofloxacin molecule have absorptions at 226 and 330 nm [30].

These functional groups in ofloxacin molecule are decomposed in photocatalytic oxidation process, which can be proven by the continuous shrinking of the absorption peaks with extending irradiation time. As stated before, the $La_2Ti_2O_7$ sample obtained using 4 g CTAB has the strongest activity on ofloxacin degradation and TOC removal efficiencies. As shown in the figure, nearly none of the absorption peaks appears in the spectrum after 120 min of photocatalytic reaction, indicating the overall destruction of the major groups in ofloxacin molecule. The quinolone substituent, benzoic ring, and piperazinyl and oxazinyl groups can all be broken up into small fragments.

Figs. 4b and c present the UV-Vis spectra of ofloxacin solution after 30 and 70 min of irradiation to show the effects of CTAB amount. The intensity reducing rates of the four major absorption peaks are in accordance to the photocatalytic activities of the materials with respect to CTAB amount. Besides the strongest absorption peak at 288 nm, the other three absorption peaks can also shrink with extending irradiation time, indicating the concurrent degradation of different groups in ofloxacin molecule.

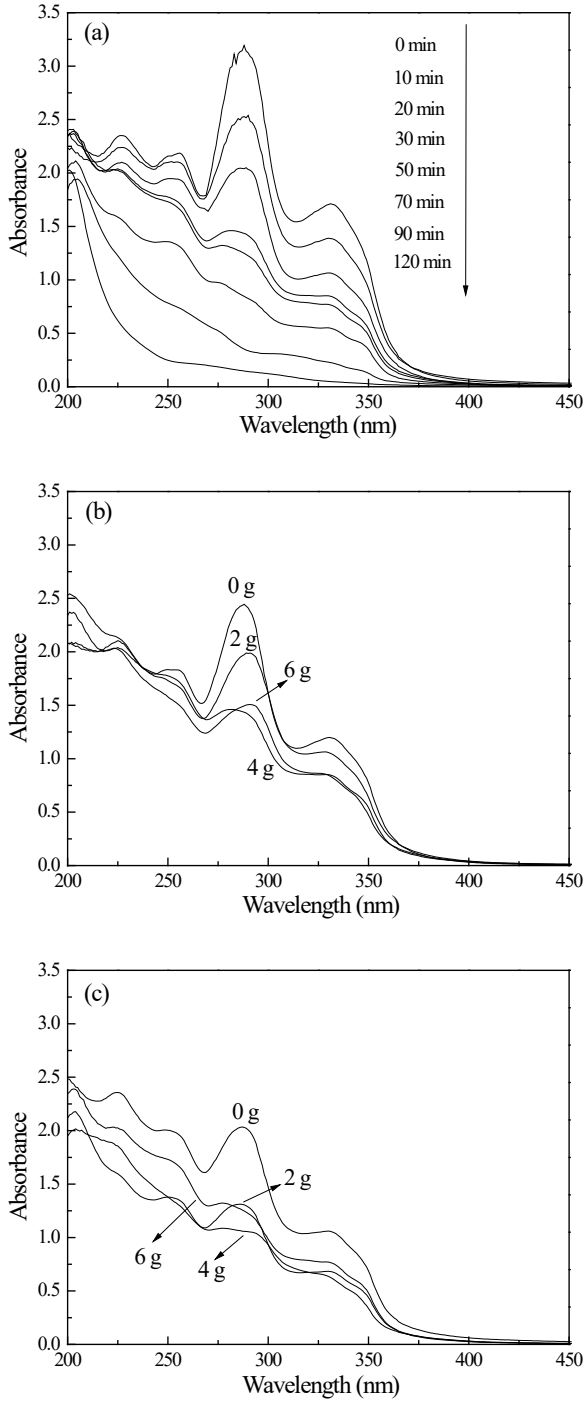

Fig. 4. (a) UV-Vis spectra of ofloxacin solution during photocatalytic degradation in presence of $La_2Ti_2O_7$ sample obtained using 4 g CTAB; UV-Vis spectra of ofloxacin solution during irradiation of (b) 30 min and (c) 70 min with respect to CTAB amount. 50 mL of 40 mg/L ofloxacin solution and 30 mg of $La_2Ti_2O_7$ were used.

Fig. 5a gives the FT-IR spectra of ofloxacin solution during photocatalytic degradation in presence of $La_2Ti_2O_7$ sample obtained using 4 g CTAB. The out-of-plane bending vibration of the conjugated double bond in quinolone substituent at 817 cm^{-1} is constantly weakened with extend-

ing reaction time. The breaking up of the conjugated double bond is measured in ultraviolet spectrum to determine the degradation efficiency of ofloxacin. The absorption at 979 cm^{-1} is due to out-of-plane bending vibration of benzene ring, which is combined with stretching vibrations of benzene ring at 1475, 1531 and 1581 cm^{-1} to indicate the existence of benzene ring [43,44]. All these absorptions of benzene ring disappear after 90 min of reaction, showing the breaking up of benzene ring.

The stretching vibration absorption of C-N bond in piperazinyl group at 1054 cm^{-1} does not change at the beginning of reaction, and its intensity may decreases after a certain time. The absorption at 1128 cm^{-1} is due to C-O bond in oxazinyl group, which is continuously reduced during photocatalytic process. The loss of absorption at 1271 cm^{-1} is attributed to the breaking up of C-F bond, showing the release of F- ions into the solution. A major oxidation intermediate, carboxylic acid, can be ascertained by the absorptions of in-plane bending vibration of O-H at 1346 cm^{-1} and C-O vibration at 1398 cm^{-1}. The esterification of carboxylic acid can lead to breaking up of O-H bond, resulting in the shrinking and disappear of the absorption peak at 1346 cm^{-1}. The absorption of carbonyl at 1621 cm^{-1} slightly shifts to high-frequency region during reaction, since the breakage of the conjugated double bond in quinolone substituent alters the bond length of carbon-oxygen double bond.

Figs. 5b and c present FT-IR spectra of ofloxacin solution after 30 and 70 min irradiation to show the effect of CTAB addition. The variation of the absorption intensity also depends on the activity of the materials. The functional groups in ofloxacin molecule are taken off during irradiation, while the decomposition of these organic groups may take longer time. It seems that the conjugated double bond in quinolone substituent can be broken at the beginning, while the other major organic groups are not decomposed. The spectra after 70 min of irradiation are obvious unique to each other due to the difference in photocatalyst activity. Nearly all the functional groups can still be found in the solution containing $La_2Ti_2O_7$ samples obtained using 0 and 2 g of CTAB, while there is only carboxylic acid existing in the solution using $La_2Ti_2O_7$ samples obtained using 4 and 6 g of CTAB.

3.3. Ionic substances in ofloxacin solution

The chemical formula of ofloxacin is $C_{18}H_{20}FN_3O_4$. Since the initial ofloxacin solution concentration is 40 mg/L, the F^- ion in the solution can be as much as 2.1 mg/L. As can be seen in Fig. 6a, the original ofloxacin contains a very small concentration of F^- ion, while fluoride ion concentration in the solution continuously increases with extending irradiation time, showing the separation of fluoride ion from ofloxacin molecule. After 120 min of irradiation, F^- ion concentration is 1.8 mg/L in the solution containing $La_2Ti_2O_7$ sample obtained without CTAB, and F^- ion concentration is as high as 2.03 mg/L in the solution using $La_2Ti_2O_7$ sample obtained with 4 g CTAB. The productivity of F^- ion is in accordance to photocatalytic activity of the prepared porous $La_2Ti_2O_7$ materials.

Figs. 6b, c and d present the variations of NH_4^+, NO_2^- and NO_3^- concentrations in the solution during ofloxacin degradation. The quinolone and piperazinyl groups in ofloxacin molecule contain nitrogen that can be degraded into the states of NH_4^+, NO_2^- and NO_3^-. As shown in Figs. 6b and c, the concentrations of NH_4^+ and NO_2^- ions constantly increase with extending reaction time. The productivities of NH_4^+ and NO_2^- ions are also in accordance to photocatalytic

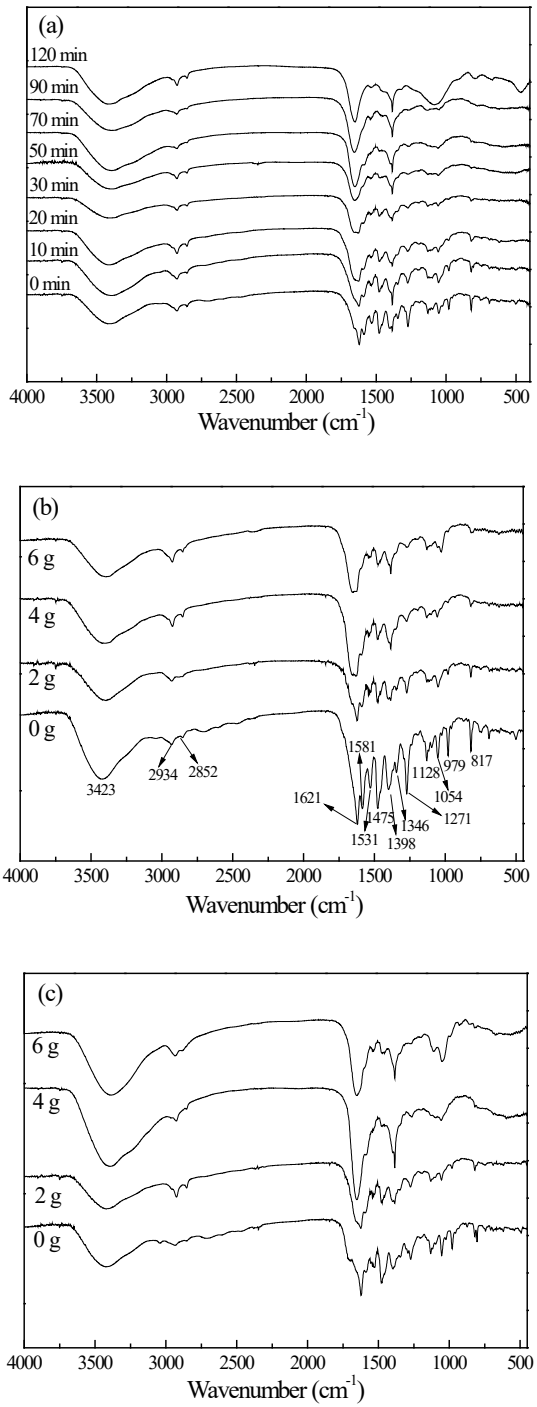

Fig. 5. (a) FT-IR spectra of ofloxacin solution during photocatalytic degradation in presence of $La_2Ti_2O_7$ sample obtained using 4 g CTAB; FT-IR spectra of ofloxacin solution during irradiation of (b) 30 min and (c) 70 min with respect to CTAB amount. 50 mL of 40 mg/L ofloxacin solution and 30 mg of $La_2Ti_2O_7$ were used.

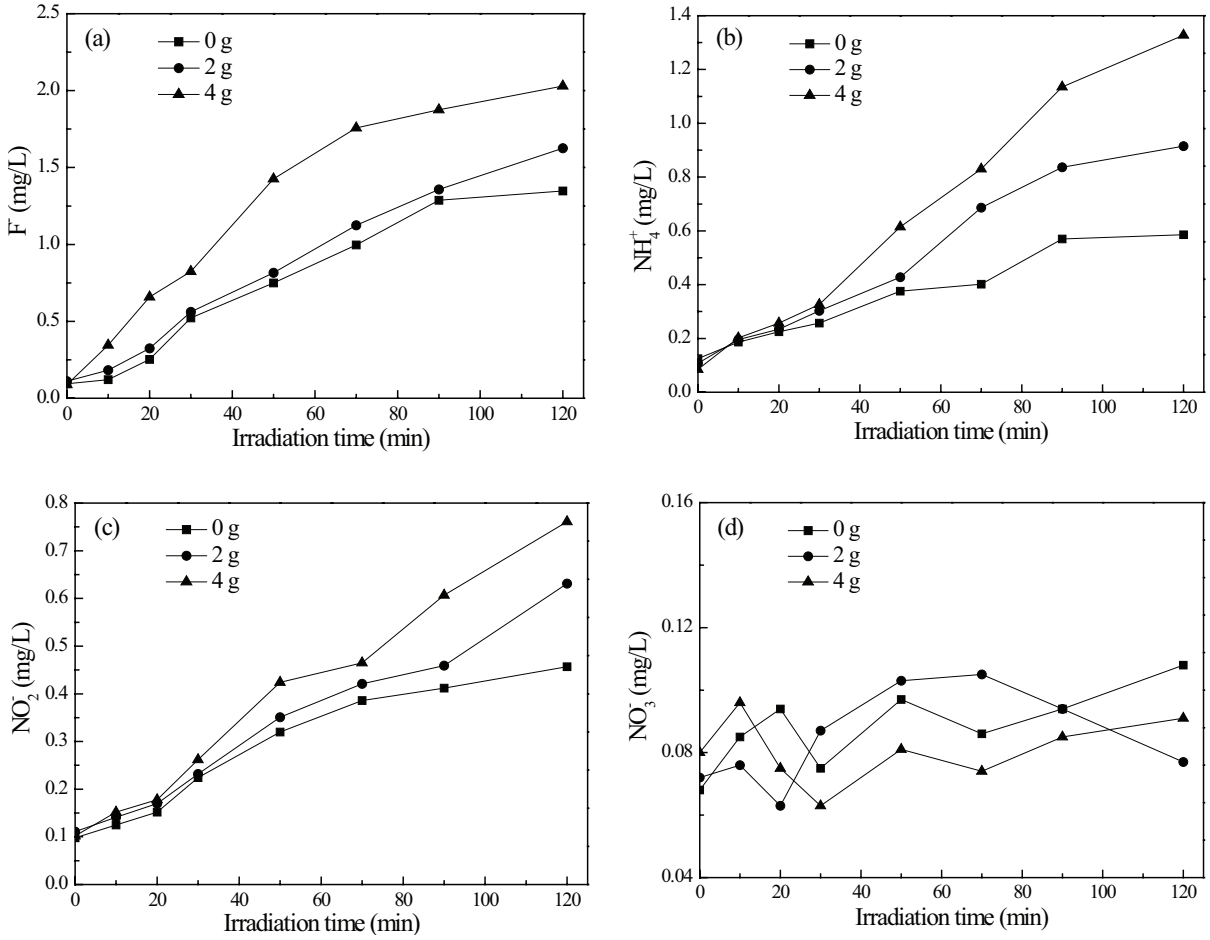

Fig. 6. Ions inofloxacin solution during degradation as a factor of CTAB amount to synthesize $La_2Ti_2O_7$. (a) F^-, (b) NH_4^+, (c) NO_2^-, (d) NO_3^-. 50 mL of 40 mg/L ofloxacin solution and 30 mg of $La_2Ti_2O_7$ were used.

activity of the prepared porous $La_2Ti_2O_7$ materials. On the other hand, as shown in Fig. 6d, the NO_3^- ion concentration is comparatively small and does not change during the whole photocatalytic degradation process. The NO_3^- ions mostly come from the free NO_3^- ions in the original ofloxacin solution and can hardly be degradation product of ofloxacin.

Fig. 7 presents the total concentration of NH_4^+, NO_2^- and NO_3^- ions inofloxacin solution during degradation. After 120 min of photocatalytic degradation, the total concentration in the solution is 2.28 mg/L when the $La_2Ti_2O_7$ sample obtained using 4 g CTAB is used as photocatalyst. On the contrary, the value is 1.15 mg/L when the $La_2Ti_2O_7$ sample obtained without CTAB is used. After the quinolone and piperazinyl groups in ofloxacin molecule are broken up, C-N bond is readily disrupted for the subsequent mineralization reaction. Since the original nitrogen concentration in 40 mg/L ofloxacin solution is 4.65 mg/L, there must be other substances containing nitrogen instead of NH_4^+, NO_2^- and NO_3^- ions. As stated before, TOC removal efficiency is 75.6% after 120 min of irradiation so that some resistant organic substances are still in the solution. Meanwhile, nitrogen can also be transformed into gaseous N_2, both dissolving in the solution and escaping into the air.

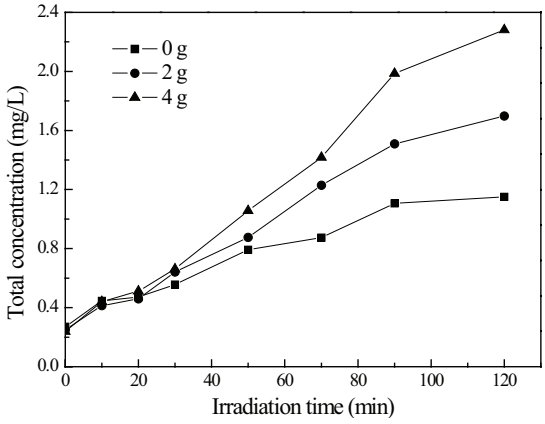

Fig. 7. Total concentration of NH_4^+, NO_2^- and NO_3^- ions inofloxacin solution during degradation. 50 mL of 40 mg/L ofloxacin solution and 30 mg of $La_2Ti_2O_7$ were used.

3.4. Photocatalytic degradation mechanism of ofloxacin

Photocatalytic degradation of organic substances starts from generation of electrons and holes after absorbing

incoming photons by photocatalyst. Firstly, the electrons and holes must migrate to the external surface of the material. The electrons can react with O_2 to produce superoxide radical anions ($^{\bullet}O_2^-$), and the holes may react with water to produce hydroxyl radicals ($^{\bullet}OH$). Superoxide anions may be recombined to generate singlet oxygen [45–47]. Organic substances such as ofloxacin can then be decomposed by the oxidative reagents.

Based on the above-mentioned experimental results, photocatalytic degradation mechanism of ofloxacin can be proposed. The breakup of C-F bond and the conjugated double bond in quinolone substituent happens at the beginning of photocatalytic degradation process. Subsequently, after the piperazinyl group is broken up, C-N bond is disrupted to release nitrogen into the solution in the forms of NH_4^+ and NO_2^-. Furthermore, C-O bond in oxazinyl group is broken up and the oxazinyl group is broken away to form benzoquinone. Finally, benzoquinone and other intermediates may be converted into butene diacid and other small carboxylic acids or esters.

4. Conclusions

Porous $La_2Ti_2O_7$ was used as photocatalyst for ofloxacin degradation to show the effects of CTAB addition. The degradation efficiency in 30 min is 35% when the $La_2Ti_2O_7$ sample obtained without CTAB is used, and it is linearly increased to 58.6% when CTAB amount is less than 4 g. Photocatalytic degradation efficiency is almost linearly enhanced with the increase of $La_2Ti_2O_7$ dosage in less than 300 mg/L. The TOC removal rate of ofloxacin solution depends on photocatalytic activity of the porous $La_2Ti_2O_7$ materials. The quinolone substituent, benzoic ring, and piperazinyl and oxazinyl groups in ofloxacin molecule can all be broken up into small fragments, while the reducing rates are in accordance to the activities of the $La_2Ti_2O_7$ material with respect to CTAB amount. The productivities of F^-, NH_4^+ and NO_2^- ions also depend on photocatalytic activity of the porous $La_2Ti_2O_7$ materials.

Acknowledgments

This work was supported by the Natural Science Foundation of Liaoning Province (No. 2015020186).

References

[1] M.R. Hoffmann, S.T. Martin, W. Choi, W. Bahnemann, Environmental applications of semiconductor photocatalysis, Chem. Rev., 95 (1995) 69–96.
[2] A. Fujishima, T.N. Rao, D.A. Tryk, Titanium dioxide photocatalysis, J. Photochem. Photobiol., C, 1 (2000) 1–21.
[3] W.J. Zhang, K.L. Wang, Y. Yu, H.B. He, TiO_2/HZSM-5 nano-composite photocatalyst: HCl treatment of NaZSM-5 promotes photocatalytic degradation of methyl orange, Chem. Eng. J., 163 (2010) 62–67.
[4] A.G. Gutierrez-Mata, S. Velazquez-Martínez, A. Álvarez-Gallegos, M. Ahmadi, J.A. Hernández-Pérez, F. Ghanbari, S. Silva-Martínez, Recent overview of solar photocatalysis and solar photo-Fenton processes for wastewater treatment, Int. J. Photoenergy, (2017), Article ID 8528063.
[5] Y.J. Wang, Q.S. Wang, X.Y. Zhan, F.M. Wang, M. Safdar, J. He, Visible light driven type II heterostructures and their enhanced photocatalysis properties: a review, Nanoscale, 5 (2013) 8326–8339.
[6] M.R. Hoffmann, S.T. Martin, W.Y. Choi, D.W. Bahnemann, Environmental applications of semiconductor photocatalysis, Chem. Rev., 95 (1995) 69–96.
[7] A. Kaur, G. Gupta, A.O. Ibhadon, D.B. Salunke, A.S.K. Sinha, S.K. Kansal, A Facile synthesis of silver modified ZnO nanoplates for efficient removal of ofloxacin drug in aqueous phase under solar irradiation, J. Environ. Chem. Eng., 6 (2018) 3621–3630.
[8] N. Arabpour, A. Nezamzadeh-Ejhieh, Modification of clinoptilolite nano-particles with iron oxide: Increased composite catalytic activity for photodegradation of cotrimaxazole in aqueous suspension, Mater. Sci. Semicond. Proces., 31 (2015) 684–692.
[9] H. Derikvandi, A. Nezamzadeh-Ejhieh, Synergistic effect of p-n heterojunction, supporting and zeolite nanoparticles in enhanced photocatalytic activity of NiO and SnO_2, J. Colloid Interf. Sci., 490 (2017) 314–327.
[10] A. Kaur, A. Umar, W.A. Anderson, S.K. Kansal, Facile synthesis of CdS/TiO_2 nanocomposite and their catalytic activity for ofloxacin degradation under visible illumination, J. Photochem. Photobiol. A: Chem., 360 (2018) 34–43.
[11] N. Ajoudanian, A. Nezamzadeh-Ejhieh, Enhanced photocatalytic activity of nickel oxide supported on clinoptilolite nanoparticles for the photodegradation of aqueous cephalexin, Mater. Sci. Semicond. Proces., 36 (2015) 162–169.
[12] H. Derikvandi, A. Nezamzadeh-Ejhieh, Designing of experiments for evaluating the interactions of influencing factors on the photocatalytic activity of NiS and SnS_2: Focus on coupling, supporting and nanoparticles, J. Colloid Interf. Sci., 490 (2017) 628–641.
[13] P. Mohammadyari, A. Nezamzadeh-Ejhieh, Supporting of mixed ZnS–NiS semiconductors onto clinoptilolite nano-particles to improve its activity in photodegradation of 2-nitrotoluene, RSC Adv., 5 (2015) 75300–75310.
[14] A. Nezamzadeh-Ejhieh, M. Khorsandi, Heterogeneous photodecolorization of Eriochrome Black T using Ni/P zeolite catalyst, Desalination, 262 (2010) 79–85.
[15] W.J. Zhang, Y.X. Liu, X.B. Pei, X.J. Chen, Effects of indium doping on properties of xIn-0.1%Gd-TiO_2 photocatalyst synthesized by sol-gel method, J. Phys. Chem. Solids, 104 (2017) 45–51.
[16] W. Zhang, Y. Liu, C. Li, Photocatalytic degradation of ofloxacin on $Gd_2Ti_2O_7$ supported on quartz spheres, J. Phys. Chem. Solids, 118 (2018) 144–149.
[17] H. Zabihi-Mobarakeh, A. Nezamzadeh-Ejhieh, Application of supported TiO_2 onto Iranian clinoptilolite nanoparticles in the photodegradation of mixture of aniline and 2, 4-dinitroaniline aqueous solution, J. Ind. Eng. Chem., 26 (2015) 315–321.
[18] A. Nezamzadeh-Ejhieh, M. Bahrami, Investigation of the photocatalytic activity of supported ZnO-TiO_2 on clinoptilolite nano-particles towards photodegradation of wastewater-contained phenol, Desal. Water Treat., 55 (2015) 1096–1104.
[19] J. Esmaili-Hafshejani, A. Nezamzadeh-Ejhieh, Increased photocatalytic activity of Zn(II)/Cu(II) oxides and sulfides by coupling and supporting them onto clinoptilolite nanoparticles in the degradation of benzophenone aqueous solution, J. Hazard. Mater., 316 (2016) 194–203.
[20] H. Derikvandi, A. Nezamzadeh-Ejhieh, A comprehensive study on enhancement and optimization of photocatalytic activity of ZnS and SnS_2: Response surface methodology (RSM), n-n heterojunction, supporting and nanoparticles study, J. Photochem. Photobiol. A: Chem., 348 (2017) 68–78.
[21] S. Jafari, A. Nezamzadeh-Ejhieh, Supporting of coupled silver halides onto clinoptilolite nanoparticles as simple method for increasing their photocatalytic activity in heterogeneous photodegradation of mixture of 4-methoxy aniline and 4-chloro-3-nitro aniline, J. Colloid Interface Sci., 490 (2017) 478–487.
[22] J. Chen, S. Liu, L. Zhang, N. Chen, New SnS_2/$La_2Ti_2O_7$ heterojunction photocatalyst with enhanced visible-light activity, Mater. Lett., 150 (2015) 44–47.

[23] W.J. Zhang, Y.J. Tao, C.G. Li, Sol-gel synthesis and characterization of $Gd_2Ti_2O_7/SiO_2$ photocatalyst for ofloxacin decomposition, Mater. Res. Bull., 105 (2018) 55–62.
[24] Z. Chen, H. Jiang, W. Jin, C. Shi, Enhanced photocatalytic performance over $Bi_4Ti_3O_{12}$ nanosheets with controllable size and exposed {001} facets for Rhodamine B degradation, Appl. Catal. B: Environ., 180 (2016) 698–706.
[25] W.J. Zhang, J. Yang, C.G. Li, Role of thermal treatment on sol-gel preparation of porous cerium titanate: Characterization and photocatalytic degradation of ofloxacin, Mater. Sci. Semicond. Process., 85 (2018) 33–39.
[26] L.M. Lozano-Sánchez, S. Obregón, L.A. Díaz-Torres, S. Lee, V. Rodríguez-González, Visible and near-infrared light-driven photocatalytic activity of erbium-doped $CaTiO_3$ system, J. Mol. Catal. A: Chem., 410 (2015) 19–25.
[27] Y.A. Zulueta, M.T. Nguyen, Multisite occupation of divalent dopants in barium and strontium titanates, J. Phys. Chem. Solids, 121 (2018) 151–156.
[28] B. Kiss, T.D. Manning, D. Hesp, C. Didier, M.J. Rosseinsky, Nano-structured rhodium doped $SrTiO_3$–Visible light activated photocatalyst for water decontamination, Appl. Catal. B: Environ., 206 (2017) 547–555.
[29] K. Katagiri, Y. Miyoshi, K. Inumaru, Preparation and photocatalytic activity of strontium titanate nanocube-dispersed mesoporous silica, J. Colloid Interface Sci., 407 (2013) 282–286.
[30] W.J. Zhang, Y.J. Tao, C.G. Li, Sol-gel synthesis of $Gd_2Ti_2O_7$/HZSM-5 composite photocatalyst for ofloxacin degradation, J. Photochem. Photobiol. A: Chem., 364 (2018) 787–793.
[31] W.J. Zhang, Z. Ma, L. Du, L.L. Yang, X.J. Chen, H.B. He, Effects of calcination temperature on characterization and photocatalytic activity of $La_2Ti_2O_7$ supported on HZSM-5 zeolite, J. Alloys Compds., 695 (2017) 3541–3546.
[32] Z.L. Hua, X.Y. Zhang, X. Bai, L.L. Lv, Z.F. Ye, X. Huang, Nitrogen-doped perovskite-type $La_2Ti_2O_7$ decorated on graphene composites exhibiting efficient photocatalytic activity toward bisphenol A in water, J. Colloid Interface Sci., 450 (2015) 45–53.
[33] Y. Zhang, C. Han, G. Zhang, D. Dionysiou, M. Nadagoudaf, PEG-assisted synthesis of crystal TiO_2 nanowires with high specific surface area for enhanced photocatalytic degradation of atrazine, Chem. Eng. J., 268 (2015) 170–179.
[34] H. Chang, E. Jo, H. Jang, T. Kim, Synthesis of PEG-modified TiO_2-$InVO_4$ nanoparticles via combustion method and photocatalytic degradation of methylene blue, Mater. Lett., 92 (2013) 202–205.
[35] W.J. Zhang, Y.J. Tao, C.G. Li, Effects of PEG4000 template on sol-gel synthesis of porous cerium titanate photocatalyst, Solid State Sci., 78 (2018) 16–21.
[36] W.J. Zhang, H.L. Li, Z. Ma, H. Li, H. Wang, Photocatalytic degradation of azophloxine on porous $La_2Ti_2O_7$ prepared by sol-gel method, Solid State Sci., 87 (2019) 58–63.
[37] A. Nezamzadeh-Ejhieh, E. Afshari, Modification of a PVC-membrane electrode by surfactant modified clinoptilolite zeolite towards potentiometric determination of sulfide, Micropor. Mesopor. Mater., 153 (2012) 267–274.
[38] M. Anari-Anaraki, A. Nezamzadeh-Ejhieh, Modification of an Iranian clinoptilolite nano-particles by hexadecyltrimethyl ammonium cationic surfactant and dithizone for removal of Pb(II) from aqueous solution, J. Colloid Interf. Sci., 440 (2015) 272–281.
[39] A. Nezamzadeh-Ejhieh, Z. Ghanbari-Mobarakeh, Heterogeneous photodegradation of 2,4-dichlorophenol using FeO doped onto nano-particles of zeolite P, J. Ind. Eng. Chem., 21 (2015) 668–676.
[40] Z. Shams-Ghahfarokhi, A. Nezamzadeh-Ejhieh, As-synthesized ZSM-5 zeolite as a suitable support for increasing the photoactivity of semiconductors in a typical photodegradation process, Mater. Sci. Semicond. Proc., 39 (2015) 265–275.
[41] S. Mousavi-Mortazavi, A. Nezamzadeh-Ejhieh, Supported iron oxide onto an Iranian clinoptilolite as a heterogeneous catalyst for photodegradation of furfural in a wastewater sample, Desal. Water Treat., 57 (2016) 10802–10814.
[42] Z.A. Mirian, A. Nezamzadeh-Ejhieh, Removal of phenol content of an industrial wastewater via a heterogeneous photodegradation process using supported FeO onto nanoparticles of Iranian clinoptilolite, Desal. Water Treat., 57 (2016) 16483–16494.
[43] K.S. Vinod, S. Periandy, M. Govindarajan, Spectroscopic [FT-IR and FT-Raman] and molecular modeling (MM) study of benzene sulfonamide molecule using quantum chemical calculations, J. Mol. Struct., 1116 (2016) 226–235.
[44] V. Arjunan, S. Thirunarayanan, S. Mohan, Energy profile analysis, spectroscopic investigations (FT–IR, FT–Raman and FT–NMR), electronic properties, structure-activity aspects and DFT studies of (1,3-benzodioxol-5-yl)acetic acid, Chem. Data Collect., 17–18 (2018) 75–94.
[45] M. Ahmadi, F. Ghanbari, Degradation of organic pollutants by photoelectro-peroxone/ZVI process: Synergistic, kinetic and feasibility studies, J. Environ. Manage., 228 (2018) 32–39.
[46] N. Jaafarzadeh, G. Barzegar, F. Ghanbari, Photo assisted electro-peroxone to degrade 2,4-D herbicide: The effects of supporting electrolytes and determining mechanism, Process Saf. Environ. Prot., 111 (2017) 520–528.
[47] Y. Nosaka, T. Daimon, A.Y. Nosaka, Y. Murakami, Singlet oxygen formation in photocatalytic TiO_2 aqueous suspension, Phys. Chem. Chem. Phys., 6 (2004) 2917–2918.